

Prediction of Concrete Cubic Compressive Strength Using ANN Based Size Effect Model

Q.W. Yang¹, S.G. Du^{1,2}

Abstract: Size effect is a major issue in concrete structures and occurs in concrete in any loading conditions. In this study, size effect on concrete cubic compressive strength is modeled with a back-propagation neural network. The main advantage in using an artificial neural network (ANN) technique is that the network is built directly from experimental data without any simplifying assumptions via the self-organizing capabilities of the neural network. The proposed ANN model is verified by using 27 experimental data sets collected from the literature. For the large specimens, a modified ANN is developed in the paper to further improve the forecast accuracy. The results demonstrate that the ANN-based size effect model has a strong potential to predict the cubic compressive strength of concrete.

Keywords: concrete; size effect; compressive strength; artificial neural network back-propagation.

1 Introduction

The size effect is a problem of scaling, which is central to every physical theory [Bazant (1999); Hoover and Bazant (2013); Chiroiu, Munteanu, and Delsanto (2010); Mustapha (2014)]. The size effect in solid mechanics is understood as the effect of the characteristic structure size (dimension) on the nominal strength of structure when geometrically similar structures are compared. Size effect is a major issue in concrete structures and occurs in concrete in any loading conditions. Kani (1967) was one of the first to demonstrate the size effect in concrete structures. It has been shown that the shear strength of similar concrete beams decreases with increasing beam depth. Manic, Taric, Serif, and Ristovski (2015) analyzes research on the formula proposed by Bazant, where the existence of size effect is shown. Alam, Kotronis, Loukili (2013) present the experimental and numerical

¹ Department of Civil Engineering, Shaoxing University, Shaoxing, 312000, P.R. China

² Corresponding author. E-mail: dushigui@126.com; Tel: +86-575-88326229; Fax: +86-575-88341503

investigations on the influence of size effect on crack opening, crack length and crack propagation. An isotropic non-local strain softening damage model is adopted for the numerical model. Sinaie, Heidarpour, Zhao, and Sanjayan (2015) carry out an experimental program to investigate the relation between size and the cyclic response of cylindrical concrete samples. The results show that diameter and the aspect ratio of the sample have the most influence on the reloading strength and reloading tangent of the cyclic response. Mahmud, Yang, and Hassan (2013) investigate the size effects on flexural strength of similar notched ultra high performance steel fibre reinforced concrete (UHPRC) beams under three-point bending tests. Both numerical and experimental studies have showed that the size effect on the nominal flexural strength of these beams up to 150mm depth is very little. Kalfat and Mahaidi (2014) present the first comprehensive experimental program into the size effect fiber reinforced polymer patch anchors. A series of uniaxial tension experiments has been conducted by van Vliet and van Mier (2000) to investigate the size effect on strength and fracture energy of concrete and sandstone. Depending on the material and the curing conditions a stronger or weaker size effect on the nominal strength occurred in the tests. The observed size effect has to be attributed to a combination of statistical size effect and strain gradients in the cross section of the specimens, which were caused by the specimen shape, load eccentricity and material inhomogeneity. Syroka-Korol and Tejchman (2014) carried out the laboratory tests on concrete beams with longitudinal bars and without shear reinforcement. A pronounced size effect was measured in these concrete beams. Ray and Kishen (2011) proposed an analytical model for estimating the fatigue crack growth in concrete by using the concepts of dimensional analysis. It is shown that the proposed fatigue law is able to capture the size effect in plain concrete and agrees well with different experimental results. Through a sensitivity analysis, it is shown that the structural size plays a dominant role followed by loading ratio and the initial crack length in fatigue crack propagation. Ashour and Kara (2014) present test results of six concrete beams reinforced with longitudinal carbon fiber reinforced polymer (CFRP) bars and without vertical shear reinforcement. A simplified, empirical equation accounting for size effect as well as all other shear design parameters was developed in their work based on the well-known design-by-testing approach. Karihaloo, Abdalla, and Xiao (2003) carry out an experimental investigation into the size effect in the strength of hardened cement paste (nominal compressive strength 40 MPa) and high strength concrete (nominal compressive strength 110 MPa) as measured in three point bending. Improvements to Karihaloo's size effect formula have been proposed in this study. Belgin and Şener (2008) present the results of full-scale failure of singly reinforced four-point-bend beams of different sizes containing deformed longitudinal reinforcing bars. The results revealed the existence of a significant size effect, which can approximately be described by the size

effect law previously proposed by Bazant. The size effect is found to be stronger in two-dimensional similarities than for one and three-dimensional similarities. Nguyen, Kim, Ryu, and Koh (2013) study the size effect on the flexural behavior of ultra-high-performance hybrid fiber-reinforced concrete (UHPHFRC). Both UHPHFRCs demonstrated clear size effect on flexural strength, normalized deflection, and normalized energy absorption capacity. Furthermore, the flexural behavior of UHPHFRC1, with its lower tensile ductility, was more sensitive to the size of the specimen. In order to investigate the size effect of concrete cubic compressive strength, Su and Fang (2014) performed a series of compression tests on 135 groups of cubic specimens with three different strength grades and three different aggregate mixtures. Test and analysis results show that the strength grade influences the size effect of concrete cubic compressive strength greatly.

The size effect in concrete is a result influenced by multi-factors, such as water/cement ratio, cement content, water content, sand ratio, maximum aggregate size, aggregate type, and other mix design parameters. According to the existing experiments, we can deduce several functions which can describe the size effect in concrete as shown in the above literatures. However, considering that the factors are too complex to be modeled and solved by classical mathematic and traditional processes, artificial neural network (ANN) may be a promising tool to accurately describe the size effect in concrete. The main benefit of an ANN-based method is that the ANN is built directly from the experimental test data without any simplifying assumptions. This paper thoroughly investigates to evaluate whether ANN can be used to forecast the size effect of concrete cubic compressive strength correctly. The ANN model is constructed, trained and tested using 27 available sets of experimental data obtained from the reference of Su and Fang (2014). The data used in ANN model are arranged in a format of seven input parameters that cover the cement (C), silica fume (SF), fine aggregate (FA), coarse aggregate (CA), water (W), superplasticizer (SP), and side length of specimen (L). The ANN model, which performs in Matlab, predicts the cubic compressive strength of the concrete. It will be shown that the ANN-based size effect model on concrete cubic compressive strength is reliable and very promising.

2 ANN-based size effect model

2.1 Background for ANN

ANN is a mathematical or computational model that tries to simulate the structure or functional aspects of biological neural networks. The first advantage of ANN is its capability of learning directly from examples, i.e. the relationships between input and output variables are generated by the data themselves. The other ad-

vantages of ANN are its accurate response to incomplete tasks, its extraction of information from noisy or poor data, and its production of generalized results from the new examples [Arslan and Ince (1996)]. Due to the above features, ANN has successfully been used in many engineering problems over the last two decades. Ince (2004) presented a fracture model based on ANN to predict fracture parameters of cementitious materials. It has been shown that the fracture model based on ANN predictions is more reliable than the Two-Parameter model based on regression analysis. Öztaş, Pala, Özbay, Kanca, Çağlar, and Bhatti (2006) used a back-propagation neural network to predict the compressive strength and slump of high strength concrete. The results showed that ANN has strong potential as a feasible tool for predicting compressive strength and slump values. Li and Yang (2008) developed a method of damage identification for beam using artificial neural network based on statistical properties of structural dynamic responses. Mehrjoo, Khaji, Moharrami, and Bahreininejad (2008) proposed a method for estimating the damage intensities of joints for truss bridge structures using a back-propagation neural network. Duan, Kou, and Poon (2013) employed an artificial neural network to predict the compressive strength of recycled aggregate concrete. Yan, Ren, Xia, Shen, and Gu (2015) developed two models to predict the two fracture parameters in the scale effect model of concrete using the artificial neural network methodology. Wang, Man, and Jin (2015) developed the artificial neural network for predicting the free expansion strain of self-stressing concrete under wet curing conditions.

Among various ANN models, the most fundamental and widely used architecture is the back-propagation neural network, which will be used in this study. As shown in Figure 1, a typical structure of the back-propagation neural network consists of an input layer, one or more hidden layers and an output layer, and each layer consists of numerous neurons. The ANN-based modeling process involves four main aspects [Duan, Kou, and Poon (2013); Yan, Ren, Xia, Shen, and Gu (2015)]: (1) data acquisition, analysis and problem representation; (2) architecture determination; (3) training of the network; and (4) validation and test of the trained network for generalization evaluation. The training process of ANN is divided into two phases. In the first phase (feed-forward), the input layer neurons pass the input pattern values onto the hidden layer. Subsequently each of the hidden layer neurons computes a weighted sum of its input, and passes the sum through its activation function and gives the activation value to the output layer. Following the computation of a weighted sum of each neuron in the output layer, the sum is passed through its activation function, resulting in one of the output values for the network. In the second stage (back-propagation), the error between actual output and target output can be calculated layer by layer in recursion and the weights are accordingly adjusted

until the expectant output is obtained in the out layer. More details on construction of ANN can be found in the references [Grossberg (1988); Hornik, Stinchcombe, and White (1989); Hornik (1991); Hornik, Stinchcombe, and White (1990); Gallant and White (1992); Oishi and Yoshimura (2007); Kerh, Lai, Gunaratnam, and Saunders (2008)].

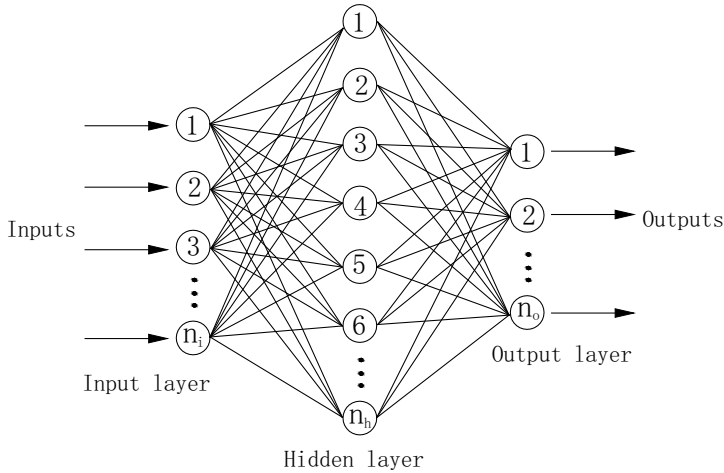


Figure 1: The architecture of the ANN model

2.2 Input and Output of the ANN

In this research, the size effect of concrete cubic compressive strength was predicted using the ANN model. Table 1 presents the experimental data taken from the existing size effect tests in the reference of Su and Fang (2014). In this experimental study, the overall dimensions of the specimens tested are as follows: $100 \times 100 \times 100$, $150 \times 150 \times 150$, and $200 \times 200 \times 200$ mm. From table 1, the seven parameters, i.e., cement (C), silica fume (SF), fine aggregate (FA), coarse aggregate (CA), water (W), superplasticizer (SP), and side length of specimen (L), are chosen as the input variables for ANN. Whereas the statistical average value of 28day compressive strength (f_{cu}) is chosen as the output variable of ANN.

2.3 Construction of the ANN

A back-propagation ANN architecture was employed in this study. As described in section 2.2, the ANN model used in this study has seven neurons (variables) in the input layer ($n_i = 7$) and one neuron in the output layer ($n_o = 1$). So far as know,

Table 1: The experimental data taken from reference Su and Fang (2014) for ANN

Specimen number	C (kg/m ³)	SF (kg/m ³)	FA (kg/m ³)	CA (kg/m ³)	W (kg/m ³)	SP (kg/m ³)	L (mm)	f_{cu} (MPa)
1-100	1140	0	0	0	661	0	100	22.10
2-100	451	0	1290	0	262	0	100	23.98
3-100	275	0	786	1179	160	0	100	25.17
4-100	1314	0	0	0	486	0	100	41.64
5-100	659	0	1098	0	244	0	100	43.30
6-100	432	0	723	1085	160	0	100	47.23
7-100	1304	238	0	0	261	26.1	100	62.21
8-100	717	129	1010	0	143	14.3	100	62.31
9-100	470	85	704	1056	94	9.4	100	70.47
10-150	1140	0	0	0	661	0	150	21.68
11-150	451	0	1290	0	262	0	150	23.48
12-150	275	0	786	1179	160	0	150	24.14
13-150	1314	0	0	0	486	0	150	40.72
14-150	659	0	1098	0	244	0	150	42.30
15-150	432	0	723	1085	160	0	150	44.21
16-150	1304	238	0	0	261	26.1	150	60.65
17-150	717	129	1010	0	143	14.3	150	60.57
18-150	470	85	704	1056	94	9.4	150	65.18
19-200	1140	0	0	0	661	0	200	21.30
20-200	451	0	1290	0	262	0	200	23.07
21-200	275	0	786	1179	160	0	200	23.18
22-200	1314	0	0	0	486	0	200	40.10
23-200	659	0	1098	0	244	0	200	41.48
24-200	432	0	723	1085	160	0	200	41.23
25-200	1304	238	0	0	261	26.1	200	59.66
26-200	717	129	1010	0	143	14.3	200	59.26
27-200	470	85	704	1056	94	9.4	200	60.18

there are no reasonable theory for determining the optimum number of hidden layers and the optimum number of neurons in each hidden layer. In this research, a single hidden layer is used in the ANN, since many investigations [Arslan and Ince (1996); Ince (2004); Öztaş, Pala, Özbay, Kanca, Çağlar, and Bhatti (2006); Li and Yang (2008); Mehrjoo, Khaji, Moharrami, and Bahreininejad (2008)] have showed that ANN with one hidden layer is sufficient to simulate most of engineering problems. As for the number of neurons in the hidden layer, too few neurons will not

allow the network to produce accurate maps from the input to the desired output, while too many neurons will result in difficulties dealing with new types of input patterns. In practice, the neuron number range of a hidden layer can be calculated by the following equation [Yan, Ren, Xia, Shen, and Gu (2015); Wang, Man, and Jin (2015)]:

$$n_h = \sqrt{n_i + n_o} + a \quad (1)$$

where n_h , n_i and n_o are the neuron number of hidden, input and output layers, respectively, and a is a fixed value ranging from 0 to 10. According to equation (1), the number of hidden layer neurons in this research can be between 3 and 13. In this research, the optimum number of neurons in the unique hidden layer is set to 11 ($n_h = 11$). The following discussion will show that when more neurons in the hidden layer are used, the network would not converge. If the network was smaller, it would not converge either.

2.4 Training and testing of the ANN

As stated before, back-propagation training algorithm is used in this ANN model. The program of the ANN model is developed and performed under MATLAB. Training and testing data of this model came from experimental results as shown in Table 1. To test the generalization ability of the ANN model, we select 9 samples with the same size as the test set, while the remaining 18 samples are used to train the network. Thus the three cases will be studied in the following.

2.4.1 Case 1: the samples with the side length of 150mm are used as the test set.

Case 1 is used to show the performance of the ANN when the test sample size ranges from the minimum size to the maximum size of the training samples. Table 2 shows the R-square results of ANN training and testing data when the neuron number of the hidden layer varies from 3 to 13. One can see from table 2 that the R-square values are both the largest when the neuron number of the hidden layer is 11 for the training and testing sets. Therefore, the neuron number of the unique hidden layer is set to 11 in this research ($n_h = 11$). As shown in figure 2, the training phase of the ANN for case 1 took 6 epochs using the given data. Figures 3 and 4 present all the experimental data, as well as the training and testing results obtained from the ANN model. The linear optimized fitted straight together with its function and the R value is shown in these figures. In addition, the mean of squared error (MSE) between the predicted value and the experimental value is also given in the title of the figure. Table 3 presents the comparison of experimental compressive strength with ANN predicted compressive strength for the testing set. From these results, one can see that the compressive strength values predicted by

the ANN model are very closer to the experimental values. It has been shown that the proposed ANN model is very accurate for predicting the compressive strength of those samples whose sizes range from the minimum size to the maximum size of the training samples.

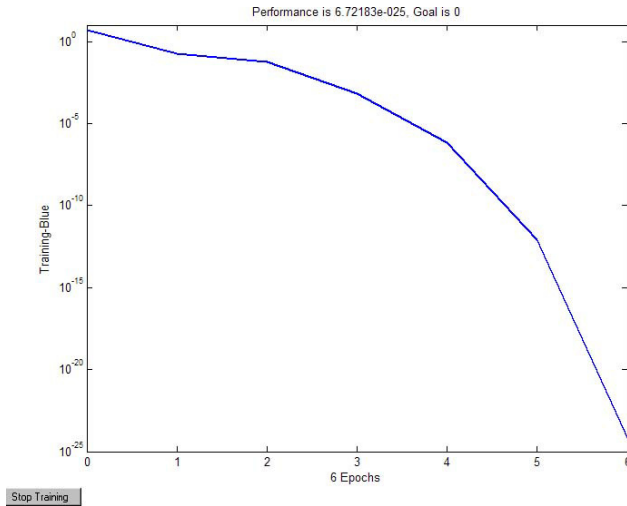


Figure 2: Variations of overall error against number of iterations for Case 1

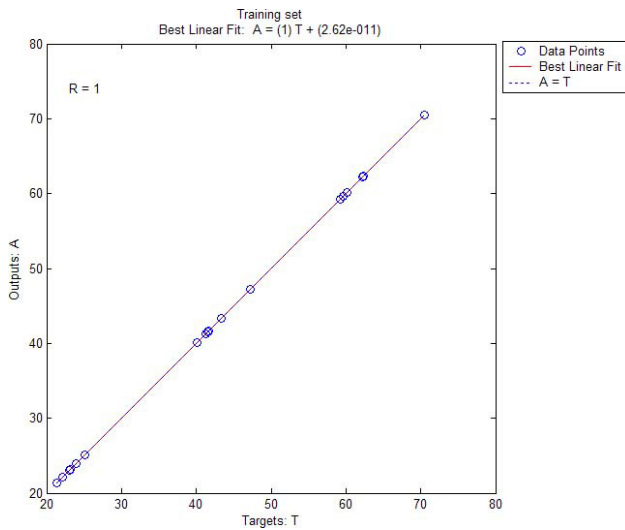


Figure 3: Performance of training set for Case 1 (MSE = 4.0629×10^{-22})

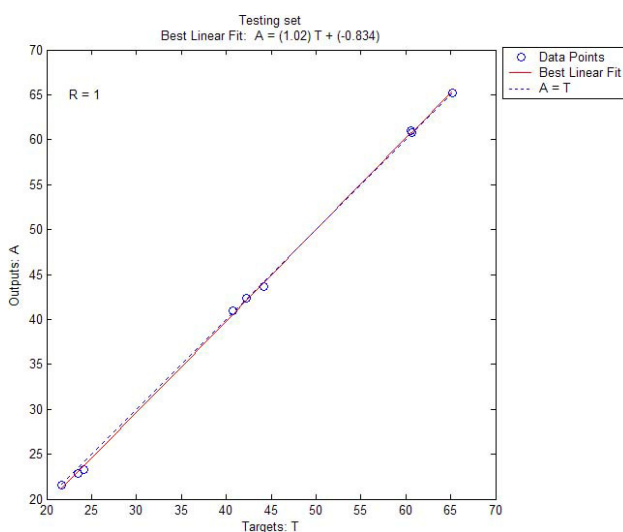


Figure 4: Performance of testing set for Case 1 (MSE = 0.1733)

Table 2: The R-square values for case 1 when the neuron number of the unique hidden layer changes

Neuron number of the hidden layer	R-square value of training set	R-square value of testing set
3	0.991	0.998
4	1	0.985
5	1	0.993
6	1	0.989
7	1	0.999
8	1	0.992
9	1	0.99
10	1	0.998
11	1	1
12	1	0.986
13	1	0.969

2.4.2 Case 2: the samples with the side length of 200mm are used as the test set.

Case 2 is used to show the performance of the ANN when the test sample size is greater than the maximum size of the training samples. As shown in figure 5, the training phase of the ANN for case 2 took 7 epochs using the given data. Figures 6 and 7 give the results for case 2 by using the ANN model. Obviously, the results show better fit in the training set than in the testing set. Table 4 presents the comparison of experimental values with ANN predicted values for the compressive

Table 3: Comparison of experimental compressive strength with ANN predicted compressive strength for testing set (Case 1)

Specimen number	Experimental values (MPa)	ANN predicted values (MPa)	Relative error (%)
10–150	21.68	21.5771	−0.47
11–150	23.48	22.9093	−2.43
12–150	24.14	23.3179	−3.41
13–150	40.72	40.9951	0.68
14–150	42.3	42.3366	0.09
15–150	44.21	43.6915	−1.17
16–150	60.65	60.8221	0.28
17–150	60.57	60.9778	0.67
18–150	65.18	65.2543	0.11

strength of testing set. Compared with the results in case 1, the prediction accuracy of the ANN for case 2 decreases. It has been shown that the generalization ability of the ANN will weaken when the test sample size is greater than the maximum size of the training samples.

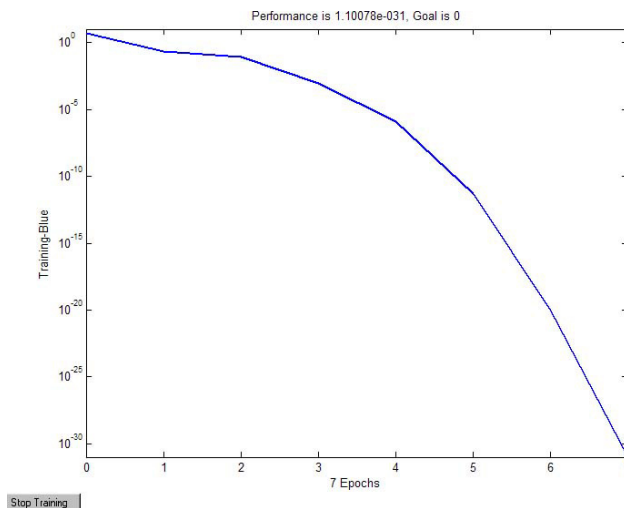


Figure 5: Variations of overall error against number of iterations for Case 2

2.4.3 Case 3: the samples with the side length of 100mm are used as the test set.

Case 3 is used to show the performance of the ANN when the test sample size is less than the minimum size of the training samples. Figures 8–10 present the

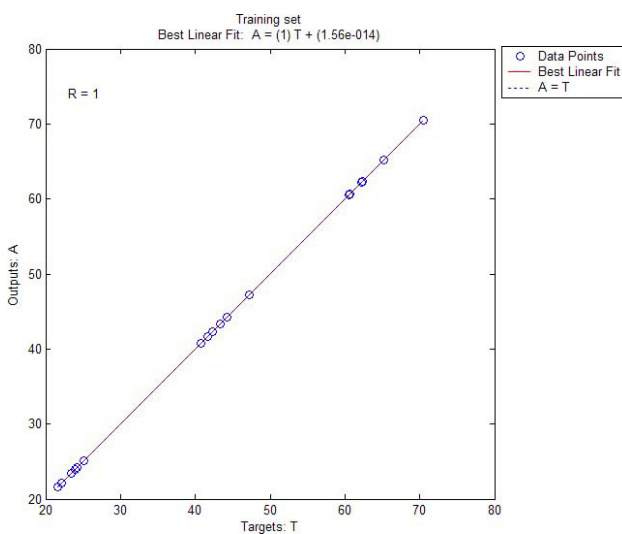


Figure 6: Performance of training set for Case 2 ($MSE = 6.5914 \times 10^{-29}$)

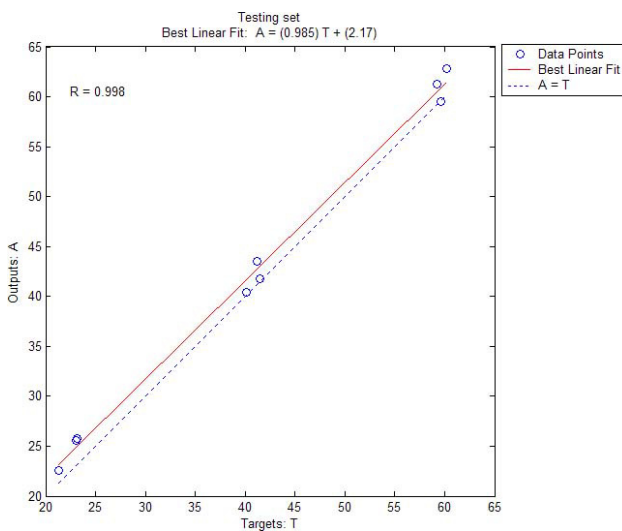


Figure 7: Performance of testing set for Case 2 ($MSE = 3.4525$)

training phase of the ANN and the results predicted by ANN. Table 5 presents the comparison of experimental values with ANN predicted values for this case. From these results, one can see that the generalization ability of the ANN also weakened when the test sample size is less than the minimum size of the training samples.

Table 4: Comparison of experimental compressive strength with ANN predicted compressive strength for testing set (Case 2)

Specimen number	Experimental values (MPa)	ANN predicted values (MPa)	Relative error (%)
19-200	21.3	22.5717	5.97
20-200	23.07	25.5604	10.8
21-200	23.18	25.817	11.38
22-200	40.1	40.3964	0.74
23-200	41.48	41.8211	0.82
24-200	41.23	43.4881	5.48
25-200	59.66	59.534	0.21
26-200	59.26	61.2736	3.4
27-200	60.18	62.8117	4.37

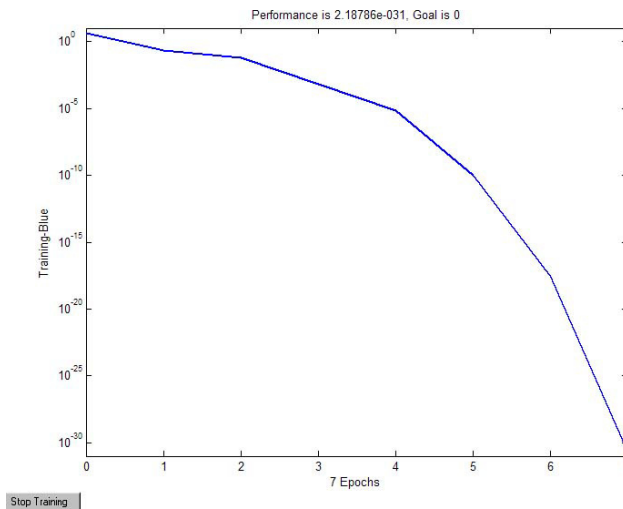


Figure 8: Variations of overall error against number of iterations for Case 3

2.5 Improvement of the ANN-base size effect model

As stated previously, the ANN is very accurate in predicting the compressive strength of the sample whose size ranges from the minimum size to the maximum size of the training samples, but not enough accurate for the other sample whose size is out of range. However, it is the most important to predict the size effect for scale ranges which can not be tested under laboratory conditions, especially for the sample whose size is far greater than the maximum size of the training samples. In view of this, a modified ANN is developed in this section to improve the forecast

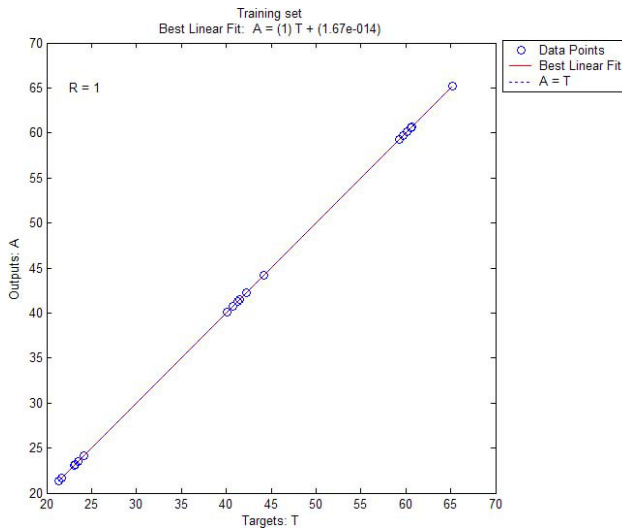


Figure 9: Performance of training set for Case 3 (MSE = 1.4796×10^{-28})

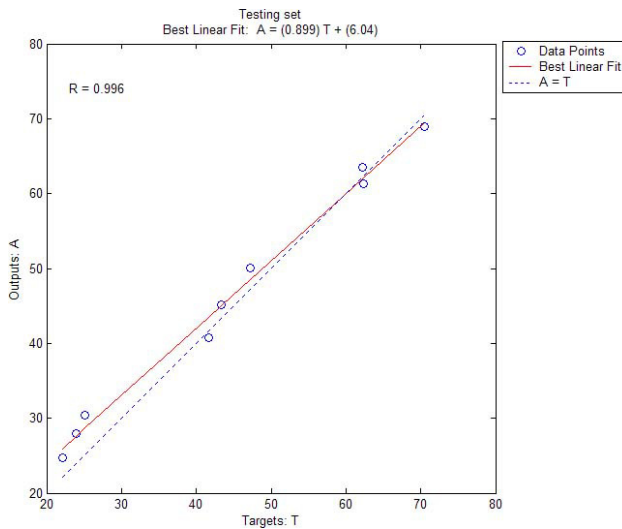


Figure 10: Performance of testing set for Case 3 (MSE = 7.3963)

accuracy for the large specimens. According to the existing theories, the size effect in concrete will significantly decline with an increase in the specimen size. Using this principle, the original ANN model in case 2 can be improved to obtain more accurate predicted values of the compressive strength for the samples with the side length of 200mm. The modifications of ANN include the following respects. First,

Table 5: Comparison of experimental compressive strength with ANN predicted compressive strength for testing set (Case 3)

Specimen number	Experimental values (MPa)	ANN predicted values (MPa)	Relative error (%)
1-100	22.1	24.684	11.69
2-100	23.98	27.9708	16.64
3-100	25.17	30.3451	20.56
4-100	41.64	40.7734	2.08
5-100	43.3	45.1748	4.33
6-100	47.23	50.0111	5.89
7-100	62.21	63.5408	2.14
8-100	62.31	61.3434	1.55
9-100	70.47	68.8964	2.23

Table 6: The nine suppositional oversized specimens

Specimen number	C (kg/m ³)	SF (kg/m ³)	FA (kg/m ³)	CA (kg/m ³)	W (kg/m ³)	SP (kg/m ³)	L (mm)	CR (%)
28-1400	1140	0	0	0	661	0	1.4 × 10 ³	0
29-1400	451	0	1290	0	262	0	1.4 × 10 ³	0
30-1400	275	0	786	1179	160	0	1.4 × 10 ³	0
31-1400	1314	0	0	0	486	0	1.4 × 10 ³	0
32-1400	659	0	1098	0	244	0	1.4 × 10 ³	0
33-1400	432	0	723	1085	160	0	1.4 × 10 ³	0
34-1400	1304	238	0	0	261	26.1	1.4 × 10 ³	0
35-1400	717	129	1010	0	143	14.3	1.4 × 10 ³	0
36-1400	470	85	704	1056	94	9.4	1.4 × 10 ³	0

in addition to all the 100 × 100 × 100 and 150 × 150 × 150 specimens, nine suppositional oversized specimens as shown in table 6 with the side length of 1400mm are added to the training set in the modified ANN. Second, the change rate (CR) of the compressive strength is used as the new output variable in the modified ANN, which is defined as the following equation:

$$CR_L = \frac{f_{cu,L-50} - f_{cu,L}}{f_{cu,L}} \times 100\% \quad (2)$$

where CR_L is the change rate of the compressive strength for the $L \times L \times L$ specimen, $f_{cu,L}$ is the cubic compressive strength of the sample with the side length of L (mm), and $f_{cu,L-50}$ is the cubic compressive strength of the sample with the

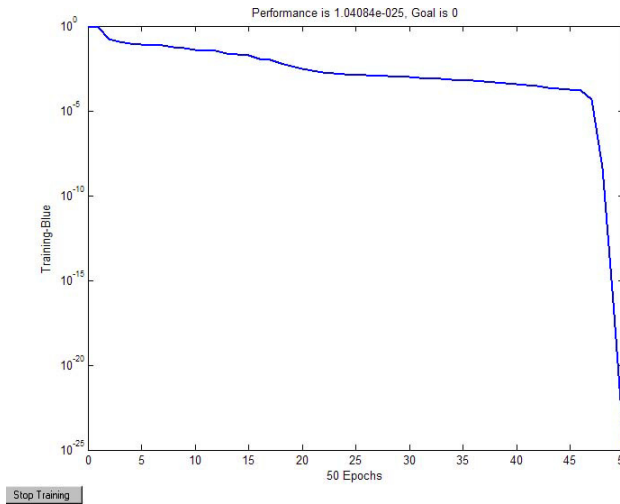


Figure 11: Variations of overall error against number of iterations for Case 2 using the modified ANN

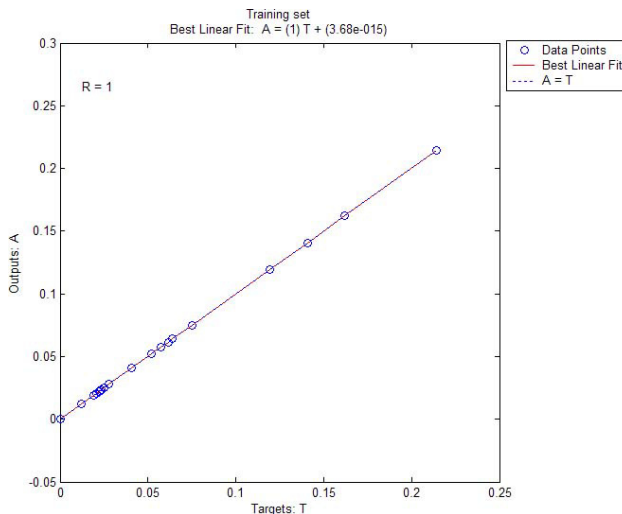


Figure 12: Performance of training set for Case 2 using the modified ANN (MSE = 1.1954×10^{-27})

side length of $(L - 50)$. For the $100 \times 100 \times 100$ specimens, the $f_{cu,50}$ used in the calculation of CR_{100} is obtained by the original ANN model. For the suppositional oversized specimens, the CR_{1400} can be set to 0 because that the size effect can be ignored for these oversized specimens. Figures 11–13 present the training phase of the modified ANN and the results predicted by the modified ANN. From figure 11, the training phase of the modified ANN for case 2 took 50 epochs using the

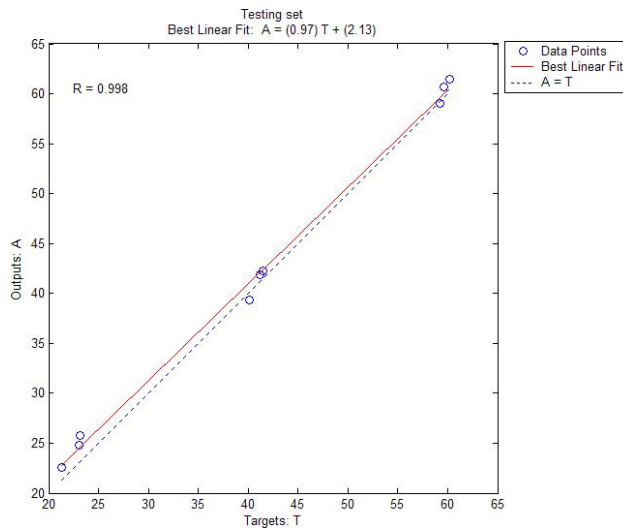


Figure 13: Performance of testing set for Case 2 using the modified ANN (MSE = 1.7069)

Table 7: Comparison of experimental values with predicted results obtained by the original and modified ANN models (Case 2)

Specimen number	f_{cu} -by experiment (MPa)	f_{cu} -by original ANN (MPa)	f_{cu} - by modified ANN (MPa)
19–200	21.30	22.5717	22.527
20–200	23.07	25.5604	24.8406
21–200	23.18	25.817	25.7229
22–200	40.10	40.3964	39.3762
23–200	41.48	41.8211	42.2209
24–200	41.23	43.4881	41.8953
25–200	59.66	59.534	60.6922
26–200	59.26	61.2736	59.0148
27–200	60.18	62.8117	61.4507

given data. Table 7 and figure 14 give the comparisons of the experimental values and the predicted ones by using the original ANN and modified ANN for these $200 \times 200 \times 200$ specimens. One can see that the predicted values obtained by the modified ANN have less error compared with the results obtained by the original ANN. In other words, the modified ANN is more accurate than the original ANN in predicting the compressive strength of the large concrete specimen.

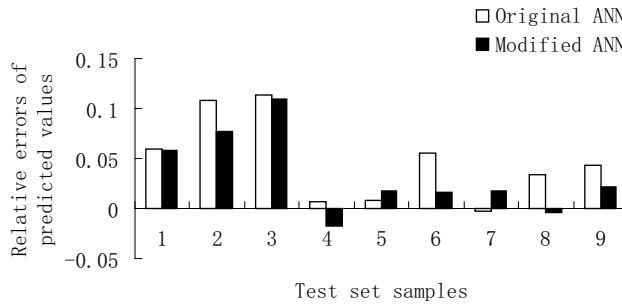


Figure 14: Comparison of the relative errors between the predicted values and experimental values by the original and modified ANN models (Case 2)

3 Conclusion

In this study, the ANN-based size effect model is assessed to see whether it can be used to predict the cubic compressive strength of the concrete. From the investigation, it can be seen that:

- (1) The proposed ANN model is very accurate for predicting the compressive strength of those samples whose sizes range from the minimum size to the maximum size of the training samples.
- (2) The generalization ability of the ANN will weaken when the test sample size is greater than the maximum size of the training samples (or less than the minimum size of the training samples).
- (3) The modified ANN is more accurate than the original ANN in predicting the compressive strength of the large concrete specimen.

In conclusion, the ANN-based size effect model has strong potential as a feasible tool for predicting the concrete cubic compressive strength in spite of some imperfections in the study of case 3. The inaccuracy in case 3 may be mainly due to a lack of enough experimental data. Therefore, the performance of ANN-based size effect model can still be improved if more experimental parameters can be considered.

Acknowledgement: This work is supported by National Natural Science Foundation of China (41427802, 11202138, 41172292) and Zhejiang Province Natural Science Foundation (LZ13D020001).

References

Alam, S. Y.; Kotronis, P.; Loukili, A. (2013): Crack propagation and size effect in concrete using a non-local damage model. *Engineering Fracture Mechanics*, vol. 109, pp. 246–261.

Arslan, A.; Ince, R. (1996): The neural network approximation to the size effect in fracture of cementitious materials. *Engineering Fracture Mechanics*, vol. 54, pp. 249–261.

Ashour, A. F.; Kara, I. F. (2014): Size effect on shear strength of FRP reinforced concrete beams. *Composites Part B: Engineering*, vol. 60, pp. 612–620.

Bazant, Z. P. (1999): Size effect on structural strength: a review. *Archive of Applied Mechanics*, vol. 69, pp. 703–725.

Belgin, Ç. M.; Şener, S. (2008): Size effect on failure of overreinforced concrete beams. *Engineering Fracture Mechanics*, vol. 75, pp. 2308–2319.

Chiroiu, V.; Munteanu, L.; Delsanto, P. P. (2010): Evaluation of the Toupin-Mindlin theory for predicting the size effects in the buckling of the carbon nanotubes. *Computers, Materials & Continua*, vol. 16, pp. 75.

Duan, Z. H.; Kou, S. C.; Poon, C. S. (2013): Prediction of compressive strength of recycled aggregate concrete using artificial neural networks. *Construction and Building Materials*, vol. 40, pp. 1200–1206.

Gallant, A. R.; White, H. (1992): On learning the derivatives of an unknown mapping with multilayer feedforward networks. *Neural Networks*, vol. 5, pp. 129–138.

Grossberg S. (1988): Nonlinear neural networks: Principles, mechanisms, and architectures. *Neural networks*, vol. 1, pp. 17–61.

Hoover, C. G.; Bazant, Z. P. (2013): Comprehensive concrete fracture tests: Size effects of Types 1 & 2, crack length effect and postpeak. *Engineering Fracture Mechanics*, vol. 110, pp. 281–289.

Hornik, K. (1991): Approximation capabilities of multilayer feedforward networks. *Neural Networks*, vol. 4, pp. 251–257.

Hornik, K.; Stinchcombe, M.; White, H. (1989): Multilayer feedforward networks are universal approximators. *Neural Networks*, vol. 2, pp. 359–366.

Hornik, K.; Stinchcombe, M.; White, H. (1990): Universal approximation of an unknown mapping and its derivatives using multilayer feedforward networks. *Neural Networks*, vol. 3, pp. 551–560.

Ince, R. (2004): Prediction of fracture parameters of concrete by artificial neural networks. *Engineering Fracture Mechanics*, vol. 71, pp. 2143–2159.

Kalfat, R.; Mahaidi, R. A. (2014): Experimental investigation into the size effect of bidirectional fiber patch anchors in strengthening of concrete structures. *Composite Structures*, vol. 112, pp. 134–145.

Kani, G. N. (1967): How safe are over large concrete beams? *ACI J. Proc.*, vol. 64, pp. 128–141.

Karihaloo, B. L.; Abdalla, H. M.; Xiao, Q. Z. (2003): Size effect in concrete beams. *Engineering Fracture Mechanics*, vol. 70, pp. 979–993.

Kerh, T.; Lai, J. S.; Gunaratnam, D.; Saunders, R. (2008): Evaluation of seismic design values in the Taiwan building code by using artificial neural network. *Computer Modeling in Engineering and Sciences*, vol. 26, pp. 1.

Leshno, M.; Lin, V. Y.; Pinkus, A.; Schocken, S. (1993): Multilayer feedforward networks with a nonpolynomial activation function can approximate any function. *Neural Networks*, vol. 6, pp. 861–867.

Li, Z. X.; Yang, X. M. (2008): Damage identification for beams using ANN based on statistical property of structural responses. *Computers & structures*, vol. 86, pp. 64–71.

Mahmud, G. H.; Yang, Z.; Hassan, A. M. T. (2013): Experimental and numerical studies of size effects of ultra high performance steel fiber reinforced concrete beams. *Construction and Building Materials*, vol. 48, pp. 1027–1034.

Manic N.; Taric M.; Serifi V.; Ristovski A. (2015): Analysis of the existence of size effect on different concrete types. *Procedia Technology*, vol. 19, pp. 379–386.

Mehrjoo, M.; Khaji, N.; Moharrami, H.; Bahreininejad, A. (2008): Damage detection of truss bridge joints using Artificial Neural Networks. *Expert Systems with Applications*, vol. 35, pp. 1122–1131.

Mustapha, K. B. (2014): Size-Dependent Flexural Dynamics of Ribs-Connected Polymeric Micropanels. *Computers, Materials & Continua*, vol. 42, no. 2, pp. 141–174.

Nguyen, D. L.; Kim, D. J.; Ryu, G. S.; Koh, K. T. (2013): Size effect on flexural behavior of ultra-high-performance hybrid fiber-reinforced concrete. *Composites Part B: Engineering*, vol. 45, pp. 1104–1116.

Oishi, A.; Yoshimura, S. (2007): A new local contact search method using a multi-layer neural network. *Computer Modeling in Engineering and Sciences*, vol. 21, pp. 93.

Öztaş, A.; Pala, M.; Özbay, E.; Kanca, E.; Çağlar, N.; Bhatti, M. A. (2006): Predicting the compressive strength and slump of high strength concrete using neural network. *Construction and Building Materials*, vol. 20, pp. 769–775.

Ray, S.; Kishen, J. M. C. (2011): Fatigue crack propagation model and size effect in concrete using dimensional analysis. *Mechanics of Materials*, vol. 43, pp. 75–86.

Sinaie, S.; Heidarpour, A.; Zhao, X. L.; Sanjayan, J. G. (2015): Effect of size on the response of cylindrical concrete samples under cyclic loading. *Construction and Building Materials*, vol. 84, pp. 399–408.

Su, J.; Fang, Z. (2014): Experimental study on impact of aggregate mixture on dimensional effect of concrete cubic compressive strength. *Journal of Building Structures*, vol. 35, pp. 152–157. (in Chinese)

Syroka-Korol, E.; Tejchman, J. (2014): Experimental investigations of size effect in reinforced concrete beams failing by shear. *Engineering Structures*, vol. 58, pp. 63–78.

Van Vliet, M. R. A.; Van Mier, J. G. M. (2000): Experimental investigation of size effect in concrete and sandstone under uniaxial tension. *Engineering Fracture Mechanics*, vol. 65, pp. 165–188.

Wang, B.; Man, T.; Jin, H. (2015): Prediction of expansion behavior of self-stressing concrete by artificial neural networks and fuzzy inference systems. *Construction and Building Materials*, vol. 84, pp. 184–191.

White, H. (1990): Connectionist nonparametric regression: Multilayer feedforward networks can learn arbitrary mappings. *Neural Networks*, vol. 3, pp. 535–549.

Yan, Y.; Ren, Q.; Xia, N.; Shen, L.; Gu, J. (2015): Artificial neural network approach to predict the fracture parameters of the size effect model for concrete. *Fatigue & Fracture of Engineering Materials & Structures*, DOI: 10.1111/ffe.12309.